

The Principle of Equivalent Obliquity and its Application to Rotary Cutting

P. K. Venuvinod and C. Rubenstein (1), Hong Kong Polytechnic/Hong Kong

J13

Hitherto it has been shown that an orthogonal rotary tool is equivalent to an oblique tool. Here a general principle of equivalent obliquity is derived which is applicable to rotary tools of any obliquity. It is shown that the general trends of the geometric features and the cutting force components observed in oblique rotary cutting can be derived using the principle of equivalent obliquity provided we know the influence of tool obliquity on (a) the chip thickness ratio and (b) the chip flow angle; these relationships having been obtained from conventional oblique cutting tests performed with a tool having the same normal rake angle as that of the rotary tool cutting the same workpiece at the same normal cutting speed. Published data obtained from conventional oblique cutting tests are used to derive expected values of chip flow angles, normal shear plane angles and cutting force components and these are shown to follow the same trends as are observed experimentally in rotary cutting. Using the principle, a number of previously puzzling phenomena observed in rotary cutting can now be explained. There are, however, features unique to rotary cutting and these are indicated.

NOMENCLATURE

b_1	Workpiece width
F	Cutting force component in the plane of the tool rake face
F_c	Cutting force component along the cutting speed direction
F_{cn}	Component of F_c perpendicular to the cutting edge in the cutting plane
F_ℓ	Component of F along the cutting edge
F_n	Component of F perpendicular to the cutting edge in the rake plane
F_t	Cutting force component normal to the machined surface
F_x	Cutting force component perpendicular to F_c and F_t
i	Static obliquity of the cutting edge
i_{eq}	Equivalent obliquity of a rotary cutting process
i_{wt}	Angular deviation between vectors V_w and V_{wt}
Q	Volume rate of metal removal
S	Shear force along the shear plane
S_ℓ	Component of S along the cutting edge
S_n	Component of S perpendicular to the cutting edge
t_1	Uncut chip thickness
t_2	Chip thickness
V_c	Chip velocity
V_{ct}	Relative velocity between the chip and the tool
V_t	Rotary speed
V_w	Work speed (cutting speed)
V_{wn}	Component of V_w perpendicular to the cutting edge in the cutting plane
V_{wt}	Relative velocity between the workpiece and the tool
W	Length of engagement of the cutting edge
Z_1, Z_2	Functions as defined in the text
α_n	Normal rake angle
η_c	Chip flow angle in rotary cutting
η_{ct}	Angular deviation of V_{ct} from the normal to the cutting edge in rake plane
η_{co}	Chip flow angle in static oblique cutting
η_n	Chip-tool friction angle in the normal plane
ξ_t	Chip thickness ratio (t_2/t_1) in rotary cutting
ξ_{to}	Chip thickness ratio (t_2/t_1) in static oblique cutting
ϕ_ℓ	Angular deviation between S and S_n
ϕ_n	Normal shear angle
τ_s	Shear stress acting on the Merchant shear plane
F_{cn}	Non-dimensional force component F_{cn} per unit length of cutting edge engagement per unit uncut chip thickness i.e. $F_{cn}/\tau_s W t_1$
F_ℓ	Non-dimensional force component F_ℓ per unit length of cutting edge engagement per unit uncut chip thickness i.e. $F_\ell/\tau_s W t_1$
F_t	Non-dimensional force component F_t per unit length of cutting edge engagement per unit uncut chip thickness i.e. $F_t/\tau_s W t_1$

INTRODUCTION

In 1952, Shaw et al [1] drew attention to the considerable similarities between the chip formation processes observed in rotary cutting and in oblique cutting. Figure 1a illustrates the rotary cutting situation investigated by them in which the cutting edge of the tool is perpendicular to the direction of cutting speed V_w - such a tool may be called an orthogonal rotary tool. Using an external rotary drive, Shaw et al imparted a tangential velocity V_t to the cutting edge. As a consequence, the moving rake surface tended to drag the chip with it so that the chip velocity vector V_c is deflected from the normal to the cutting edge in the rake plane by an angle η_c .

The chip sliding velocity V_{ct} is given by the vector equation

$$\bar{V}_{ct} = \bar{V}_c - \bar{V}_t \quad (1)$$

as illustrated in Figure 1b where η_{ct} is the deviation of the chip sliding velocity vector \bar{V}_{ct} from the normal to the cutting edge in the rake plane. Using experimental results obtained by varying the rotary speed ratio V_t/V_w in the range 0 to 2, Shaw et al showed that the relationship between the magnitudes of $\arctan(V_t/V_w)$ and η_{ct} was similar to that between obliquity i and chip flow angle η_c obtained in conventional static oblique cutting under similar cutting conditions. As a result, they suggested that the rotary cutting process at a given V_t/V_w could be considered as equivalent to a conventional oblique cutting process with the equivalent obliquity i_{eq} being given by

$$i_{eq} = \arctan(V_t/V_w) \quad (2)$$

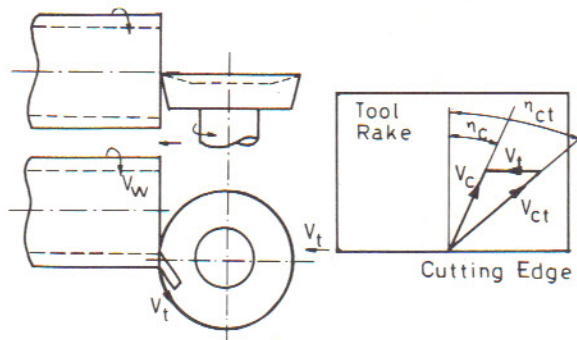


Fig. 1a Orthogonal Rotary Cutting

1b Velocity Configuration at Tool Rake

Several years later, Venuvinod et al [2-5] made a detailed study of the influence of the rotary speed ratio on the geometry, kinematics and mechanics of chip formation in oblique rotary tools. Thus, the behaviour observed with orthogonal rotary tools (studied earlier by Shaw et al) is a particular case, when $i = 0$, of the more general form of rotary cutting. In addition, they investigated the effect of varying the rotary speed ratio over a wide range (-100 to +100). Figure 2a shows the experimental set up used in these studies. It may be noted that, for the purpose of establishing consistency with equations developed in the present paper, the convention used in Figure 2a for defining the positive and negative directions of V_t is opposite in sense to that reported in [2-5]. For the purpose of characterising the combined influence of obliquity i and rotary speed ratio, Venuvinod et al used a parameter i_{wt} defined as the angular deviation of the vector V_{wt} representing the relative velocity between the workpiece and the tool from the cutting speed vector V_w . The magnitude of i_{wt} was obtained from a vector diagram similar to that shown in Figure 2b which represents the obvious relationship

$$\bar{V}_{wt} = \bar{V}_w - \bar{V}_t$$

(3)

The parameter i_{wt} , however, proved to be neither an elegant nor a comprehensive means of explaining the various experimental observations on oblique rotary cutting and it was necessary to resort to rather cumbersome arguments such as distinguishing between the ranges of 'medium' and 'high' rotary speed ratios. It was suggested that, in the 'medium' rotary speed range, the rake surface of the tool (moving at velocity V_t) tended to carry the chip with it so that the chip flow angle η_c decreased as V_t was increased in the positive direction (see Figure 2a) whereas η_c increased when V_t was increased in the negative direction. Again, it was suggested that there ought to be a limit within which the chip flow angle η_c could respond to changes in V_t so that eventually a condition would be reached when the chip would begin sliding at significantly higher velocities relative to the rake surface and hence the frictional drag at the chip tool interface was expected to fall significantly. This drop in frictional drag was invoked to explain the observed rapid increase in normal shear angle ϕ_n and the conspicuous decrease in the magnitudes of the cutting force components at large absolute magnitudes of rotary speed ratio.

While the arguments described above are plausible the resulting picture of oblique rotary cutting is far too complex and leaves a feeling that some key factor is missing from the arguments put forth. It will be shown in the present work that a general principle of equivalent obliquity, applicable to oblique rotary cutting, can be developed and that this is the factor that has been missing in modelling rotary cutting. It will be shown that this principle is capable of predicting, broadly, the effect of rotary speed on chip geometry, chip kinematics and the cutting force components obtained in oblique rotary cutting. The only experimental data required in order to effect this prediction is the influence of the angle of obliquity on the chip thickness ratio and on the chip flow angle observed when a static oblique tool is used to cut the same work material using the same tool geometry, the same uncut chip thickness and the same normal component of cutting speed, V_{wn} . It will be demonstrated that the use of the generalised principle of equivalent obliquity renders the analysis of oblique rotary cutting much more elegant and straight forward than hitherto realised. However, it will also be shown that there are inherent limitations which render the search for accurate quantitative prediction abortive.

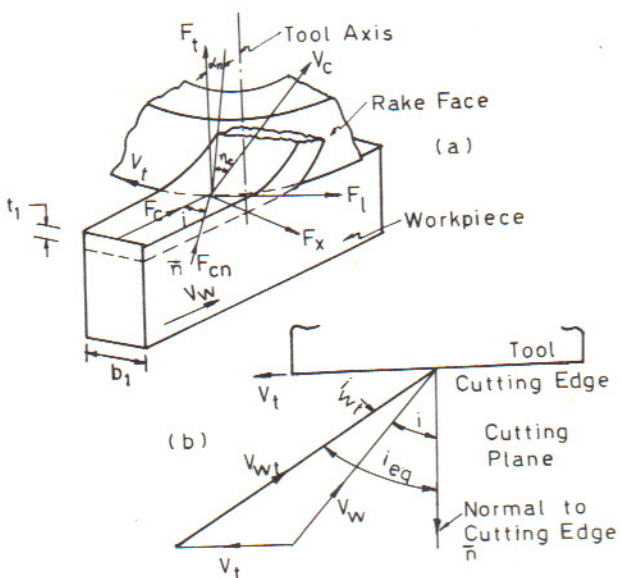


Fig. 2a Oblique Rotary Cutting
b Velocity Configuration in the Cutting Plane

GENERALISATION OF THE PRINCIPLE OF EQUIVALENT OBLIQUITY

In conventional oblique cutting with a static tool, obliquity i is defined as the angular deviation of the cutting speed vector \bar{V}_w from \bar{n} , the normal to

the cutting edge in the cutting plane. Such a definition is adequate as long as the tool is static i.e. $i_{wt} = 0$. However, in the presence of a finite rotary speed V_t , the relative velocity between the workpiece and the tool is no longer collinear with \bar{V}_w . Consequently, the obliquity may be re-defined in more general terms as the angle between the relative velocity vector \bar{V}_{wt} (between the workpiece and the tool) and \bar{n} .

Henceforth, the obliquity so defined will be referred to as the equivalent obliquity, i_{eq} , which is to be distinguished from the static obliquity i .

The magnitude of i_{eq} can be calculated easily from the velocity configuration at the cutting plane as illustrated in Figure 2b. As seen from the figure

$$i_{eq} = i + i_{wt} \quad (4)$$

where

$$i_{wt} = \arctan \left[\frac{(V_t/V_w)\cos i}{1 + (V_t/V_w)\sin i} \right] \quad (5)$$

Thus the equivalent obliquity of a rotary process is the sum of two component obliquities viz the static obliquity i and the kinematic obliquity i_{wt} . It may be noted that when $i = 0$ (i.e. orthogonal rotary tool) equation (5) reduces to equation (2) proposed by Shaw et al [1]. It is possible to appreciate now why the use of i_{wt} as the basic parameter for the explanation of various empirical trends in rotary cutting by Venuvinod et al [2 - 5] did not lead to a simple picture of rotary cutting. The factor overlooked in their analysis is the recognition of the sum ($i + i_{wt}$) as the basic parameter rather than i_{wt} itself. This is evident from the fact that when the rotary speed ratio V_t/V_w is varied from $-\infty$ to $+\infty$ in equations (4) and (5), i_{wt} varies in the range $(90-i)^\circ$ to $-(90+i)^\circ$ whereas i_{eq} varies from -90° to $+90^\circ$ irrespective of the magnitude of i .

Consider now the velocity configuration at the rake surface (Figure 1b). In static oblique cutting the chip flow angle η_{co} is defined as the angular deviation of the chip velocity vector \bar{V}_c from the normal to the cutting edge in the rake plane. In the presence of a rotary speed, however, this definition is inadequate since the relative velocity \bar{V}_{ct} between the chip and the tool is no longer collinear with the chip velocity \bar{V}_c . However, if we replace \bar{V}_c by \bar{V}_{ct} in the above definition we conclude that the equivalent chip flow angle in rotary cutting is given by the angular deviation of the relative chip velocity vector \bar{V}_{ct} from the normal to the cutting edge - a definition valid for all forms of rotary cutting including orthogonal rotary cutting ($i = 0$).

Suppose now that we perform a set of rotary cutting tests using several values of tool obliquity, i , and that we vary the speed ratio for each obliquity angle. If this concept of equivalent obliquity is valid, all of the data points generated by these experiments should lie about one chip flow, η_{ct} , - equivalent obliquity, i_{eq} , curve, independent of tool obliquity. Data generated in this way were presented against i_{wt} [4] and the resulting curves are reproduced in Figure 3a. For comparison these data are re-presented as η_{ct} versus i_{eq} in Figure 3b and they can be seen to lie about a single curve, thus lending support to the validity of this concept of equivalent obliquity.

THE CONDITIONS OF EQUIVALENCE

A corollary to the concept of equivalence is that the normal cutting plane corresponding to a rotary cutting process is identical to the normal cutting plane of the equivalent static oblique cutting process so that resolving velocities onto the normal planes shown in Figures 1b and 2b, we obtain

$$V_{wn} = V_w \cos i = V_{wt} \cos i_{eq} \quad (6)$$

$$\text{and } V_{cn} = V_c \cos \eta_c = V_{ct} \cos \eta_{ct} \quad (7)$$

A further requirement for equivalence is that the workpiece removal rate, Q , in the equivalent cutting process must be the same as that in the rotary cutting process. If, in addition, we wish to ensure the equivalence of any size or slenderness ratio effects which might be present then we require that the uncut chip thickness, t_1 , the cutting edge engagement length, W , and the normal component of the cutting speed V_{wn} be the same.

$$\text{Then } Q = V_{wb} t_1 = V_{wn} W t_1$$

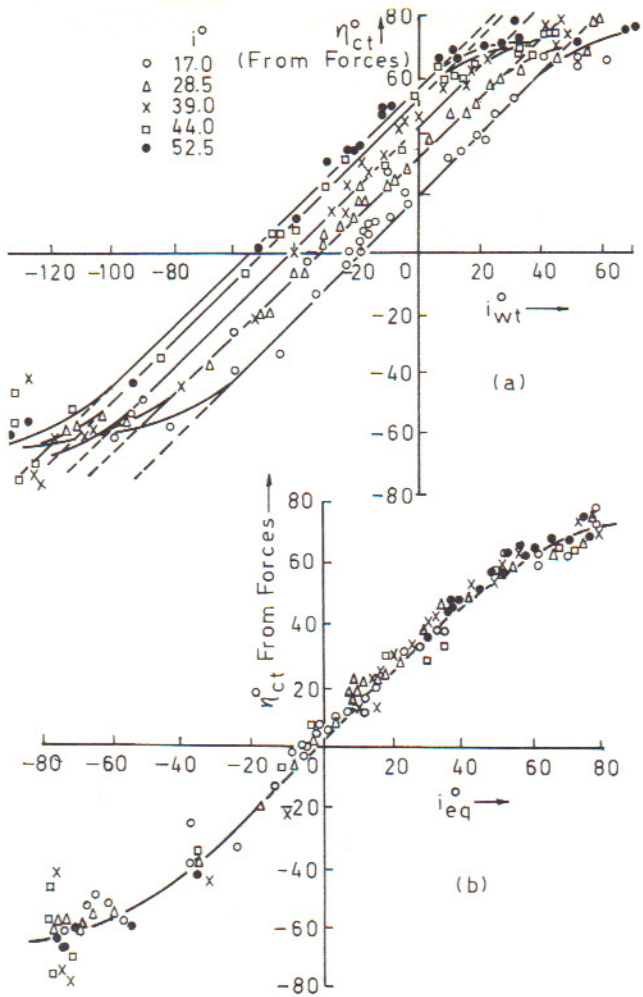


Fig. 3a Variation of η_{ct} with i_{eq} in Rotary Machining

b Variation of η_{ct} with i_{eq} while
Rotary Machining ($t_1 = 0.1\text{mm}$,
 $b_1 = 6\text{mm}$, $\alpha_n = 17$ to 21° ,
 $V_w = 0.2\text{m/min}$, workpiece copper)

where $W = b_1/\cos i$

However, even if we were to adopt an obliquity angle i_{eq} and the requisite values of cutting speed, uncut chip thickness and cutting edge engagement length, complete equivalence would still evade us since in static oblique cutting the chip contacts the tool over the same patch of the rake face while in rotary cutting new areas of the rake face continuously contact the chip. As a consequence, whereas oily contaminant and oxide films are destroyed in the first few moments of static oblique cutting, these layers are continuously replenished in rotary cutting thus modifying chip/tool adhesion. Hence, in general, chip/tool adhesion can be expected to be less in rotary cutting than it is in static oblique cutting - only when the speed ratio is zero (i.e. $i_{eq} = i$) will the chip/tool adhesion in rotary cutting be equal to that occurring in static oblique cutting.

This, however, is not the only difference between rotary and static oblique cutting. At very low speed ratios there is an insignificant increase in energy input yet there is a significant increase in the volume of tool material into which heat generated at the chip/tool interface can be conducted - consequently we can anticipate a drop in rake face temperatures as i_{eq} deviates from i . A reduction in temperature produces an increase in chip/tool adhesion so that this effect would oppose the influence of replenishment. This cooling effect can be expected to be significant, however, only at high cutting speeds. In contrast, at very high speed ratios, considerable heat may be generated at the chip/tool interface [4] which may result in the generation of a fluid layer at the interface [6]. Finally, when the speed ratio $\sim \sin i$ (i.e. $i_{eq} = 0$) a unique chip having a triangular cross-section is produced [5]; yet another feature unparalleled in static oblique cutting.

In the light of these not inconsiderable differences it would seem that little of value could be derived by applying the principle of equivalent obliquity to static oblique cutting data - surprisingly we find that the broad behaviour trends observed in rotary cutting can be predicted. To achieve this objective we assume, first, that complete equivalence exists and then we amend the picture to allow for the anticipated effects of the deviations from complete equivalence which have just been described.

THE IDEALISED CONDITION OF PERFECT EQUIVALENCE

Suppose that the functional relationship between the chip flow angle, η_{co} , and tool obliquity, i , is known from static oblique cutting experiments and that this can be expressed as

$$\eta_{co} = Z_1(i)$$

and, similarly, that the dependence of chip thickness ratio, ξ_{to} on obliquity angle is known and can be expressed as

$$\xi_{to} = Z_2(i)$$

If perfect equivalence could be established this would include identity of chip/tool interface conditions and then we would have, by definition,

$$\eta_{ct} = Z_1(i_{eq}) \quad (8)$$

$$\text{and } \xi_t = Z_2(i_{eq}) \quad (9)$$

As an example of the application of these concepts, consider the prediction of the chip flow angle, η_c , occurring in a rotary cutting process. From the velocity configuration in Figure 1b it can be seen that

$$V_t = V_{cn}(\tan \eta_{ct} - \tan \eta_c) \quad (10)$$

$$\text{However, } V_{cn}/V_{wn} = t_1/t_2 = 1/\xi_t \quad (11)$$

So that combining equations (5), (6) and equations (8) - (11) we obtain

$$\begin{aligned} \tan \eta_c &= \tan \eta_{ct} - \frac{\xi_t \tan i_{wt}}{\cos i (\cos i - \tan i_{wt} \sin i)} \\ &= \tan Z_1(i_{eq}) - \frac{Z_2(i_{eq}) \tan i_{wt}}{\cos i (\cos i - \tan i_{wt} \sin i)} \end{aligned} \quad (12)$$

Thus, assuming that perfect equivalence exists, equation (12) expresses the predicted dependence of the chip flow angle in rotary cutting on tool obliquity and on speed ratio. If, in addition, we make the assumptions that cutting edge force components are negligible, that the chip is formed by shear at a single shear plane and that the shear force on the shear plane and the force component on the rake face are collinear with and opposite in sense to the shear velocity and the relative chip velocity in these planes, respectively, then we can predict all the parameters listed in the appendix by using equation (12) to predict η_c and then using equations (A1) to (A15).

In Figures 4-6 the predicted influence of changes in i_{eq} on the chip flow angle, η_c , the normal Merchant shear plane angle, ϕ_n , and the non-dimensional cutting force components per unit length of tool engagement per unit uncut chip thickness \bar{F}_{cn} , \bar{F}_t and \bar{F}_g are shown. This has been accomplished by taking Zorey's empirical data [7] obtained by cutting 20Kh steel using static oblique cutting process and deriving therefrom empirical expressions for $Z_1(i)$ and $Z_2(i)$. It follows then that the curves shown in Figures 4-6 are predictions of the behaviour to be anticipated if 20Kh steel were to be cut by a rotary machining process provided complete equivalence were to be attained.

ALLOWANCE FOR THE EFFECTS OF IMPERFECT EQUIVALENCE

As an example, consider the variation of \bar{F}_{cn} with i_{eq} shown in Figure 6 and reproduced as curve (a) in Figure 7. This curve results from the assumption, inter alia, that the chip/rake face friction conditions in rotary cutting are exactly those obtaining in static oblique cutting. However, as has been mentioned above, except when conditions correspond to $i_{eq} = i$, the friction conditions in rotary cutting would be less severe because of replenishment of oxide and contaminant layers on that part of the rake face at which the chip contacts the tool. A reduction in tool/chip adhesion will cause a reduction in the cutting force components so that the curve which allows for a reduction in the severity of

tool/chip adhesion will lie entirely below curve (a) but can be expected to show similar characteristics. Thus, by allowing for the replenishment effect, the dependence of \bar{F}_{cn} on i_{eq} is represented by curve (b) which lies below curve (a) everywhere except at $i_{eq} = i$ at which point there is no replenishment effect. Finally, in the vicinity of $i_{eq} = 0$ the tool becomes self-propelled and chips of triangular cross-section are produced [5] - this clearly involves a different chip formation process from that by which rectangular chips are formed. It would be remarkable if both formation processes were equally energetically demanding so that we can expect some discontinuity in the vicinity of $i_{eq} = 0$. Curve (b) in Figure 7 is the composite curve depicting the anticipated variation of \bar{F}_{cn} with i_{eq} . Similarly a discontinuity in the vicinity of $i_{eq} = 0$ and a peak in the vicinity of $i_{eq} = i$ are to be anticipated when the influence of i_{eq} on \bar{F}_t is examined. In contrast, we note that the force component along the cutting edge, F_g , will be zero at $i_{eq} = 0$ irrespective of the magnitude of tool/chip adhesion so that we do not anticipate a discontinuity around $i_{eq} = 0$ when the variation of \bar{F}_g with i_{eq} is examined although, of course, a peak around $i_{eq} = i$ will still be present.

In the same way, increased tool/chip adhesion will cause the chip thickness to increase and hence the normal shear plane angle, ϕ_n , to decrease so that in the vicinity of $i_{eq} = i$ we might expect values of ϕ_n to be lower than those which would be anticipated if ideally perfect equivalence were to occur, while, as before, in the vicinity of $i_{eq} = 0$ we can expect a discontinuity. When, however, we come to consider the dependence of chip flow angle on equivalent obliquity we find that it is impossible to make an unequivocal prediction of the effect to be anticipated from an increase in tool/chip adhesion since this would cause both η_{ct} and ξ_t to increase and reference to equation (12) shows that there is no way of deciding what would be the net effect of these changes on η_c .

COMPARISON WITH EXPERIMENTAL OBSERVATION

It is clear from the above discussion that in view of the many imponderables involved, there is no way in which an accurate quantitative prediction of rotary cutting parameters could be made from static oblique cutting data. The most we could hope to predict and hence, explain, would be the qualitative behaviour to be observed in rotary cutting.

Accordingly there is no particular benefit to be derived from performing static oblique cutting tests on, say, a copper workpiece in order to predict the trends to be anticipated when copper is cut in a rotary machining process. If, as is the case, static oblique cutting data obtained by cutting steel have been published then these data can be used to make qualitative predictions which can then be compared with results obtained when copper is cut by a rotary machining process.

In Figure 4 the variation of the chip flow angle, η_c , with the equivalent obliquity angle i_{eq} as predicted from Zorev's data obtained when 20Kh steel was cut in a static oblique machining operation at $V_w = 0.7\text{m/min}$, $t_1 = 0.2\text{mm}$ and $\alpha_n = 20^\circ$ with H.S.S. tools [7] is shown. This is to be compared with the predicted relation between the same parameters derived from data obtained from the rotary oblique cutting of

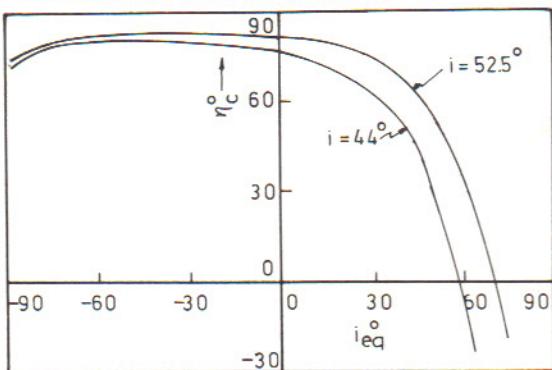


Fig. 4 Predicted Variation of η_c with i_{eq} Assuming Complete Equivalence (Zorev's Data [7])

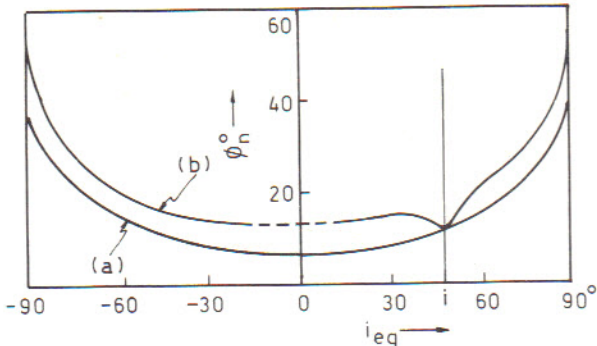


Fig. 5 Predicted Variation of ϕ_n with i_{eq}

(a) Assuming Complete Equivalence

(b) Allowing for Variation in Tool/Chip Adhesion

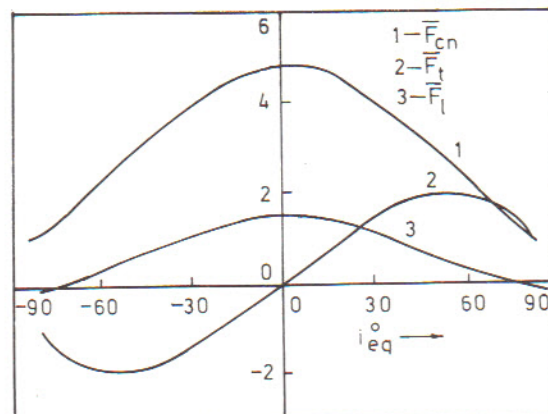


Fig. 6 Predicted Dependence of Non-dimensional Cutting Force Components Per Unit Length of Cutting Edge Engagement Per Unit Uncut Chip Thickness with i_{eq} ($i = 0 - 70^\circ$). Assuming Complete Equivalence (Data after Zorev [7], Machining, 20Kh steel, HSS tool, $V_w = 0.7\text{m/min}$, $t_1 = 0.2\text{mm}$ and $\alpha_n = 20^\circ$)

copper [2-4] depicted in Figure 8. It is immediately obvious that

- (i) there is a remarkable similarity between the predicted and empirically observed trends,
- (ii) data obtained when adopting a higher value of tool obliquity, i , lie entirely above those appropriate to a lower value of i - in complete accord with prediction
- (iii) there is little evidence in the vicinity of $i_{eq} = 0$ and $i_{eq} = i$ of any systematic deviation of the experimental data from the trend depicted in Figure 4 which was predicted on the assumption of ideally perfect equivalence. The chip flow angle is, perhaps, the cutting parameter which we might anticipate would be least affected by changes in tool/chip adhesion since $\tan \eta_c$ is expressed as the difference of two terms (vide equation (12)) both of which

increase as tool/chip adhesion increases.

(iv) the change in the sign of the slope of the η_c versus i_{eq} characteristic in the region of high negative values of i_{eq} can now be seen to occur simply as a consequence of the difference in the rates of change (with i_{eq}) of the two terms appearing in equation (12) - each of which changes monotonically with i_{eq} . Accordingly it is not necessary to invoke the cumbersome though plausible arguments detailed in the introduction in order to explain this observation.

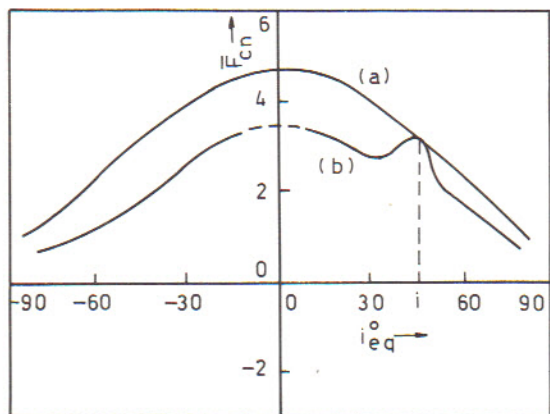


Fig. 7a Assuming Complete Equivalence (Zorev's Data [7])

b Allowing for Variation in Chip/Tool Adhesion

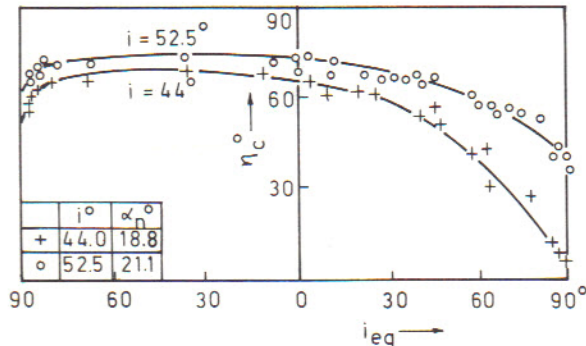


Fig. 8 Empirical Variation of η_c with i_{eq} (Cutting Conditions as in Fig. 10a)

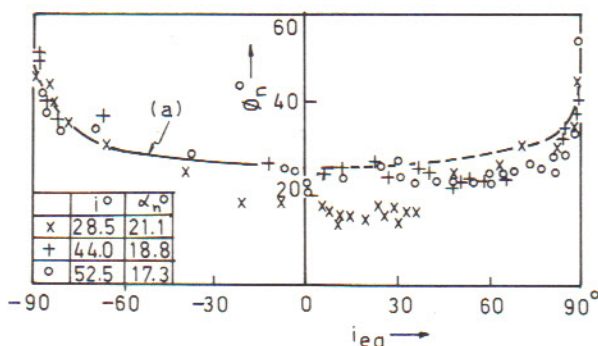


Fig. 9 Measured Variation of ϕ_n with i_{eq}

— Curve (a) drawn through experimental points in range $-90^\circ > i_{eq} > -10^\circ$
 ---- Mirror image of curve (a) which would be expected if complete equivalence were to exist. (Cutting Conditions as in Fig. 10a)

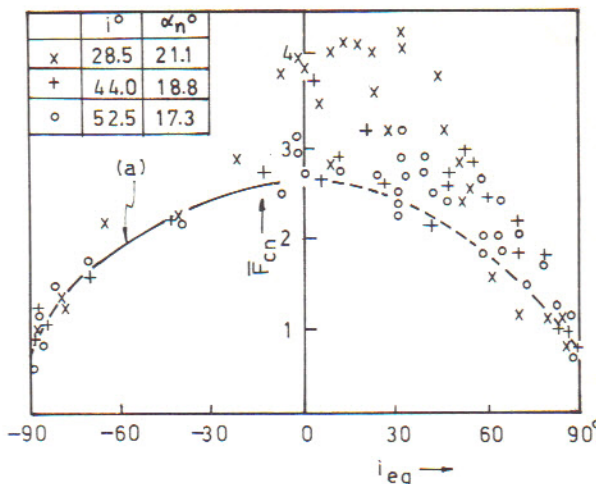


Fig. 10a Empirical Relation between \bar{F}_{cn} and i_{eq}

— Curve (a) drawn through experimental points in range $-90^\circ > i_{eq} > -10^\circ$
 ---- Mirror image of curve (a) which would be expected if complete equivalence were to exist. (Workpiece copper, $V_w = 0.2\text{m/min}$, $t_1 = 0.1\text{mm}$, $b_1 = 6\text{mm}$)

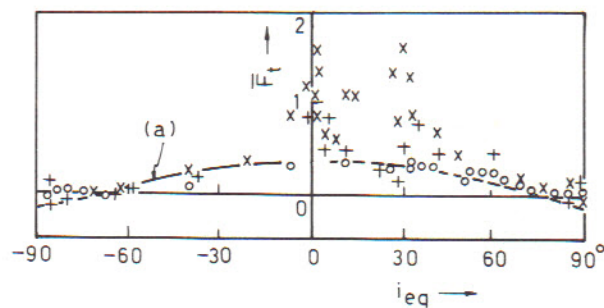


Fig. 10b Empirical Relation between \bar{F}_t and i_{eq} . (Cutting Conditions and Symbols as in Fig. 10a)

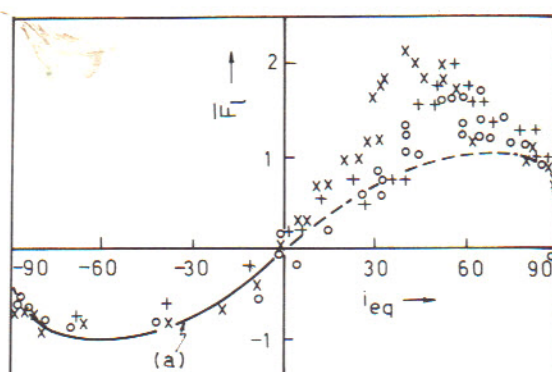


Fig. 10c Empirical Relation between \bar{F}_l and i_{eq} . (Symbols and Cutting Conditions as in Fig. 10a, Significance of Curve (a) and Dashed Curve is as in Fig. 10a)

In Figure 5, the anticipated variation of the normal Merchant shear plane angle, ϕ_n , with i_{eq} is shown and, for comparison, the relation derived from data obtained from rotary cutting tests performed on copper is depicted in Figure 9. While there is no clear evidence of distinct peaks around $i_{eq} = 0$ and $i_{eq} = i$, it should be noted that where the experimental data deviate from the curve which would be predicted by ignoring any change in tool/chip adhesion around $i_{eq} = 0$ and $i_{eq} = i$, these deviations are (i) systematically towards lower values of ϕ_n and (ii) occur, predominantly in the domain $i_{eq} > 0$ - both of which observations are entirely consistent with the model proposed in this paper. Since, in the vicinity of $i_{eq} = 0$ the measured values of ϕ_n are reduced we may conclude that the triangular chip corresponds to a condition of increased tool/chip adhesion which, if true, should result in the discontinuity in the force components F_{cn} and F_t in the vicinity of $i_{eq} = 0$ being in the form of peaks rather than troughs.

In Figures 10a, 10b there is clear evidence of peak deviations in the force components F_{cn} and F_t in the vicinity of $i_{eq} = 0$ and in the vicinity of $i_{eq} = i$ - exactly in accordance with expectation. In contrast, Figure 10c shows that, as expected, there is no peak around $i_{eq} = 0$ when \bar{F}_t is presented against i_{eq} although peaks in the vicinity of $i_{eq} = i$ are to be seen.

CONCLUSIONS

From the considerations detailed above, the following conclusions may be drawn :

1. Geometric and kinematic equivalence between a rotary cutting process and a static oblique cutting process can be established if, in the latter process
 - (i) the angle of tool obliquity is chosen to be equal to the angular deviation of the vector representing the relative velocity between the workpiece and the tool from the normal to the cutting edge in the cutting plane and
 - (ii) the uncut chip thickness, the cutting edge engagement length and the normal component of the cutting speed are chosen so as to be equal to their respective values in the rotary cutting process.
2. Using the empirical relationships between (i) the chip flow angle and tool obliquity and (ii) the chip thickness ratio and tool obliquity as determined in a static oblique cutting process and then making allowance for anticipated variations in tool/chip adhesion in rotary machining, it is possible to predict the qualitative behaviour of cutting parameters associated with chip formation and cutting forces in rotary machining. This qualitative prediction can be made everywhere except in the vicinity of $i_{eq} = 0$.

ACKNOWLEDGEMENT

The authors wish to thank the Directors of Shiu Wing Steel Limited, Hong Kong for their generosity in providing financial support for the work described in the present paper.

REFERENCES

1. Shaw, M.C., Smith, P.A., and Cook, N.H., "The Rotary Cutting Tool," Trans. A.S.M.E., Vol. 74, pp 1065-1076, Aug 1952.
2. Venuvinod, P.K., Analysis of Rotary Cutting Tools, PhD Thesis, University of Manchester Institute of Science and Technology, Manchester, 1971.
3. Venuvinod, P.K., Reddy, P.N., and Barrow, G., "New Discoveries Widen the Scope of Rotary Machining", Proc. Int. Conf. Prodn Eng., New Delhi, Vol. I, pp 243-252, Aug 1977.
4. Venuvinod, P.K., Lau, W.S., and Reddy, P.N., "Some Investigations into Machining with Driven Rotary Tools", J. Eng. Ind., Trans. A.S.M.E., Vol. 103, pp 469-477, Nov 1981.
5. Venuvinod, P.K., and Reddy, P.N., "Some Studies on Cutting with Self Propelled Rotary Tools", Paper No. 81-WA/Prod-16, Winter Annual Meeting of A.S.M.E., Washington, Nov 1981.
6. Venuvinod, P.K., Lau, W.S., and Reddy, P.N., "On the Formation of a Fluid Film at the Chip Tool Interface in Rotary Machining", submitted for presentation at 1983 CIRP General Assembly, Harrogate, U.K.
7. Zorev, N.N., Metal Cutting Mechanics, Pergamon Press, 1966.

APPENDIX

Parametric Equations Used in the Prediction of the Performance of Oblique Rotary Cutting

$$\phi_n = \arctan \left(\frac{\cos \alpha_n}{\xi_t - \sin \alpha_n} \right) \quad (A.1)$$

$$\phi_\ell = \arctan \left(\frac{\tan i \cos(\phi_n - \alpha_n) - \sin \phi_n \tan \alpha_n}{\cos \alpha_n} \right) \quad (A.2)$$

$$S = \frac{\tau_s W_t}{\sin \phi_n} \quad (A.3)$$

$$S_n = S \cos \phi_\ell \quad (A.4)$$

$$S_\ell = S \sin \phi_\ell \quad (A.5)$$

$$F_\ell = S_\ell \quad (A.6)$$

$$F_n = F_\ell \cot \alpha_n \quad (A.7)$$

$$\theta_n = \arctan \left\{ \frac{\cos(\phi_n - \alpha_n)}{\frac{S_n}{F_n} + \sin(\phi_n - \alpha_n)} \right\} \quad (A.8)$$

$$F_{cn} = \frac{S_n \cos(\theta_n - \alpha_n)}{\cos(\phi_n + \theta_n - \alpha_n)} \quad (A.9)$$

$$F_t = F_{cn} \tan(\theta_n - \alpha_n) \quad (A.10)$$

$$F_c = F_{cn} \cos i + F_\ell \sin i \quad (A.11)$$

$$F_x = F_\ell \cos i - F_{cn} \sin i \quad (A.12)$$

$$\bar{F}_t = F_t / \tau_s W_t \quad (A.13)$$

$$F_{cn} = F_{cn} / \tau_s W_t \quad (A.14)$$

$$F_{cn} = F_{cn} / \tau_s W_t \quad (A.15)$$

Note : Explanations for the symbols used above are available in the Nomenclature.

